communications earth & environment

Article

https://doi.org/10.1038/s43247-024-01397-5

Pre-failure operational anomalies of the Kakhovka Dam revealed by satellite data

Qing Yang[1], Xinyi Shen[1] ✉, Kang He[2], Qingyuan Zhang[3,4], Sean Helfrich[4], William Straka III[5], Josef M. Kellndorfer[6] & Emmanouil N. Anagnostou[2]

On June 6, 2023, the Kakhovka Dam in Ukraine experienced a catastrophic breach that led to the loss of life and substantial economic values. Prior to the breach, the supporting structures downstream of the spillway had shown signs of being compromised. Here, we use multi-source satellite data, meteorological reanalysis, and dam design criteria to document the dam's pre-failure condition. We find that anomalous operation of the Kakhovka Dam began in November 2022, following the destruction of a bridge segment, which led to persistent overtopping from late April 2023 up to the breach, contributing to the erosion of the spillway foundation. Moreover, our findings also highlight safety and risk-reduction measures pivotal in avoiding such scenarios. To help prevent future disasters, we advocate for greater transparency in the design parameters of key water structures to enable risk management, and conclude that remote sensing technology can help ensuring water infrastructure safety.

Effective monitoring and forecasting of water-related hazards are of paramount importance to ensure societal and environmental sustainability. Remote sensing has emerged as a potent tool for hazard monitoring[1–3] and assessment[4–7], particularly in data-poor or access-restricted regions[8]. Despite this technique's unique ability to unveil insights into the integrity of water infrastructure[9,10], detect operational anomalies, and identify early warning signs of structure compromise[11], comprehensive case studies that demonstrate emergency response application on actual events remain scant.

On June 6, 2023, the Kakhovka Dam in Ukraine experienced a catastrophic breach. The environmental loss was approximated at 1.2 billion euros[12], with at least 62 human lives lost, hundreds injured, and up to 100,000 individuals displaced[13]. These consequences were compounded by a near-total loss of irrigation systems in the agricultural sector following the disruption of four major canals fed by the Kakhovka reservoir, which in 2021 had enabled the harvest of approximately four million tons of crop products worth about $1.5 billion[14]. Rebuilding the dam is projected to require at least five years and ~$1 billion[15], a stark illustration of the aftermath of such disasters. Various reports and studies have documented damage inflicted by missiles, shelling, or mines on bridges, piers, and even sluice gates at the dam site[16]. These war-related impacts, compounded by anomalous reservoir regulation and spring flood conditions, led to the lowest and highest water levels ever recorded[17,18]. Before the breach, the supporting structures downstream of the activating spillway started to show signs of being compromised[19]. These reports warrant an in-depth analysis to elucidate the factors contributing to the dam's pre-failure condition, which may have exacerbated downstream flood damage post-breach, with the ultimate aim of identifying preventive measures to avoid such dangerous states.

In this study, we synergized multi-sourced remote sensing data, meteorological reanalysis products, and the dam design parameters to detect anomalous reservoir operation, estimate overflow conditions, and identify signs of potential structure compromise. We outlined possible safety checkpoints and proposed potential risk-mitigation strategies. Our objective is to underscore the utility of remote sensing data for water infrastructure monitoring by proposing new technical standards to effectively identify operational anomalies and irregularities. This approach bolsters the early warning capacity for water hazards, particularly in regions with limited access to traditional monitoring systems.

Results and discussion

Identification of irregular operation and structure compromise

Upon meticulous examination of multi-sourced optical images during the period from 2017 to 2023, we pinpointed the inception of the Kakhovka Dam's anomalous operations starting on November 11, 2022.

[1]School of Freshwater Sciences, University of Wisconsin-Milwaukee, Milwaukee, WI, USA. [2]Department of Civil & Environmental Engineering, University of Connecticut, Storrs, CT, USA. [3]Earth System Science Interdisciplinary Center, University of Maryland, College Park, MD, USA. [4]Center for Satellite Applications and Research, National Oceanic and Atmospheric Administration, College Park, MD, USA. [5]Cooperative Institute for Meteorological Satellite Studies, University of Wisconsin-Madison, Madison, WI, USA. [6]Earth Big Data LLC, Woods Hole, MA, USA. ✉e-mail: xinyis@uwm.edu

As demonstrated in Fig. 1a, the conventional operation of the spillway sluice gates predominantly occurred in early summer, with activation varying from around 30–80% and typically lasting for a duration of less than 2 months, a pattern characteristic of flood mitigation. However, from November 2022 onwards for over 6 months, the spillway activation percentage remained approximately constant, 15% of the total capacity, and the activated gates of the spillway remained the same (Fig. 2c–f). Consequently, in 2023, the reservoir dropped to the lowest in late January and escalated to the highest water level in April, respectively, compared with the same period of the past three decades (Fig. 1c), and while the water levels of the other reservoirs in the Dnipro cascade remained within reasonable ranges (Supplementary Fig. 1). Figure 2a, b shows a damaged segment of the bridge to the river's right bank on November 11, 2022. Around 3 days later, a limited number of gates near the left bank were activated (Fig. 2c). Furthermore, the outflow rate of the dam can be approximated as a function of the water level from November 2022 to June 2023, whereas such an approximation did not hold over the 2017–2022 period (Fig. 3a). This may indicate that effective regulation has been absent since November 2022, which can be confirmed in the tests ending in as early as the first week of January.

The spillway banks began overtopping around April 23, 2023 (Fig. 2d), and the estimated outflow through the activated spillway surpassed the designed capacity by April 22, 2023 (Fig. 3b). Subjected to a month-long overflow condition, the spillway ancillary structure exhibited visible damage to the pier on the downstream side of the opening gates by May 28, 2023, as revealed by ultra-high-resolution Maxar images[19]. The curved bridge and its supporting structures on the same location of the spillway began to show signs of compromise on June 2, 2023 (Fig. 2e), with additional parts missing by June 4 (Fig. 2f). This sequence of events highlights that the pattern of damage to the spillway during the pre-failure period was likely attributable to erosion at the spillway foundation, resulting from the extended period of overflow[20–22].

Safety checkpoints and mitigation measurements

As listed in Table 1, the initial safety checkpoint would be November 11, 2022, when the damage inflicted upon the sluice gates likely undermined the

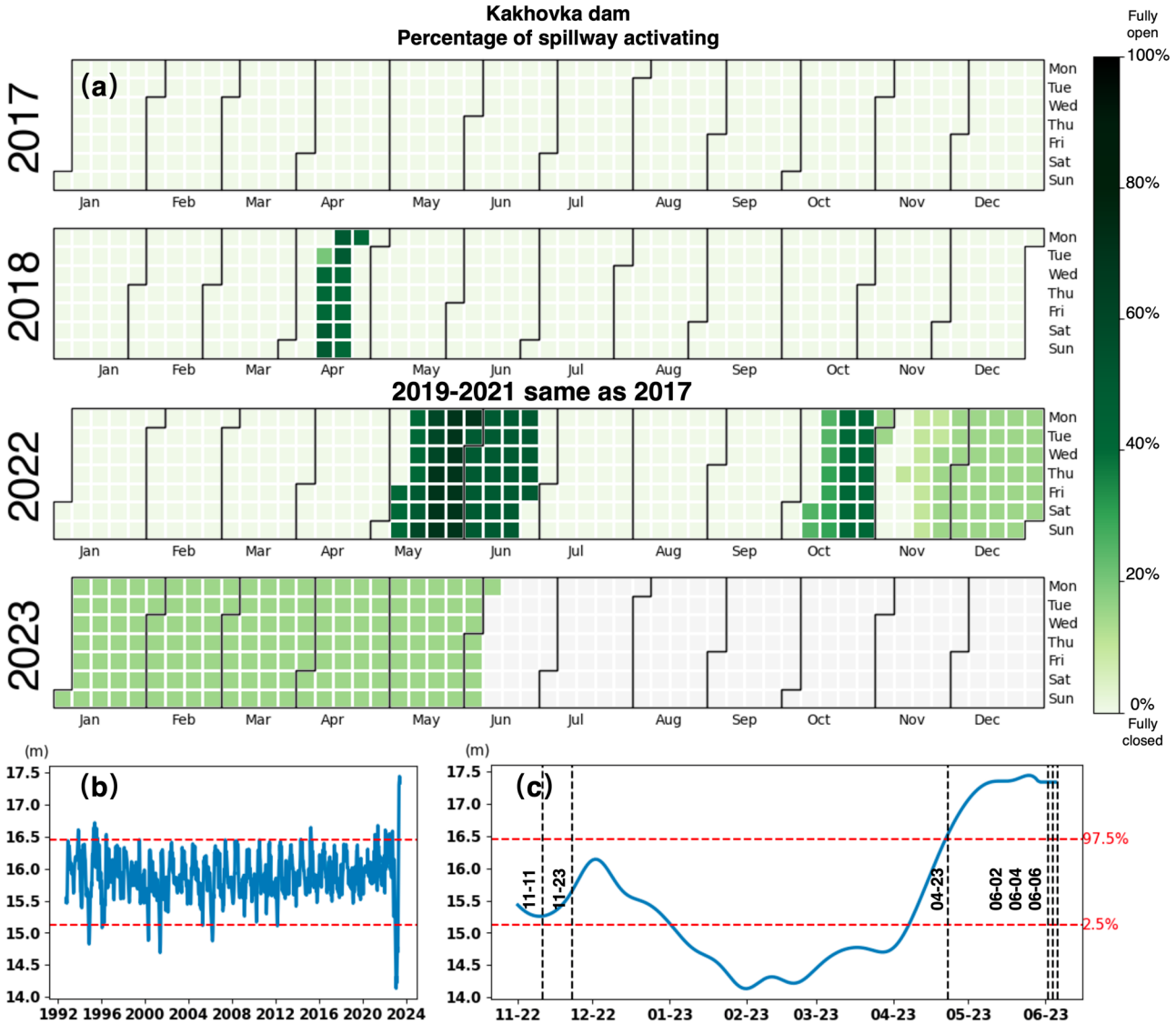

Fig. 1 | The identification of operational anomalies of Kakhovka Dam using remote sensing data. a Daily activation percentage of spillways from 2017 to 2023: darker shades represent a higher percentage of activated spillways. **b** The cubic spline interpolated, and 7-day average smoothed reservoir water-level series over 1992 to 2023, in EGM2008 datum. **c** Water-level time series zoom-in during the pre-failure period, with sequential event time marks observed from PlanetScope images: right bank bridges missing (11–11), spillway activation fixed at 15% (11–23), right bank gates overtop (04–23), left bank bridges compromised (06–02), additional left bank parts missing (06–04), and dam breach (06–06).

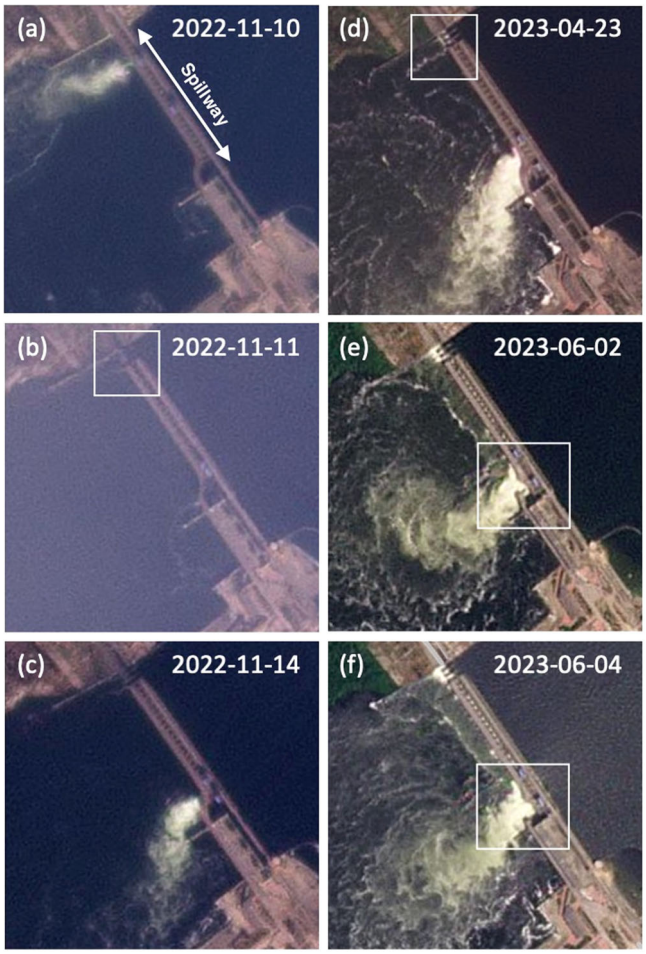

Fig. 2 | Monitoring of spillway activation on key dates illustrated through PlanetScope images. a, **b** Before and after bridge damage near the right bank of the spillway on November 11, 2022. **c** Small portion of the spillway activated on November 14, 2022. **d** The spillway structure started overtopping on April 23, 2023. **e** The bridge near the left bank began to show signs of compromise on June 2, 2023. **f** Additional parts were missing by June 4, 2023. The white polygons represent the focus areas of anomaly events. The white arrow in (**a**) indicates the extent of the spillway structure. Image © 2022–2023 Planet Labs PBC.

dam's performance for flood protection. The subsequent checkpoint emerged on January 31, 2023, when it became clear that the dam's outflow is unregulated, potentially resulting in a low water level that poses a threat to water resource safety. The third checkpoint likely surfaced on February 28, 2023, due to the sustained usage of the same portion of spillway which could bring about or accelerate the loss of structural integrity. The fourth checkpoint was on March 31, 2023, when the water level commenced its upward trend, and the estimated probability of overtopping, under the conditions of observed spillway activation, reached 23%. Given the dam was already overtopping based on PlanetScope image (Fig. 2d), the fifth checkpoint on April 23, 2023, signals an emergency state, with the risk of persistent hazardous conditions pegged at 79% in the absence of corrective measures. The final checkpoint presented itself on May 28, 2023, when visible structural compromises were confirmed, with a predicted likelihood of 45% of the dam remaining in an overtopping state in June in the absence of action.

The proposed mitigation strategy for the early stages (from November 2022 to February 2023) is of minor to moderate intensity. Restorative actions such as repair of the damaged sluice gates or maintenance of others could have ensured the functionality of flood reduction. Even without comprehensive repairs, implementing control mechanisms such as the deployment of management personnel or preemptive water release by partially activating more spillways in March 2023 could have curtailed the likelihood of overtopping. Opportunities for mitigating overtopped conditions also remained, contingent on the operational state of the spillway during the later stages (from April to May 2023). Furthermore, preventative actions should be implemented in the potentially affected regions, commencing with flood warnings and subsequent evacuations, which could have mitigated impacts.

Dam management in war conditions

A series of conspicuous anomalies and signs of neglect, observed since November 11, 2022, likely contributed to the overtopping condition of the Kakhovka Dam, which might have intensified the flood damage downstream after the breach. Despite the visible damage, when disregarded, the spillway outflow should still uphold more than 80% of its designed capacity [23]. Nonetheless, our analysis might indicate that the reservoir operations utilized a scant 10% of the total design capacity. It should be noted that the issue of overtopping was unlikely to be rectified by intensifying cascade regulation, given that from January to May 2023, the upstream reservoirs' storage capacities were occupied by over 8.5 cubic kilometers of water (Fig. 3b), constituting over 80% of the current usable volume. The peculiar reservoir operation stirred concerns by local media before and during the spring flood season[18,24], yet no effective countermeasures were implemented to mitigate the risk. Furthermore, as the dam began to show signs of impending structure damage, there was a conspicuous absence of a hazard warning, implying a possible violation of safety procedures and disaster prevention protocols.

In a war situation, ensuring the safety of the reservoir infrastructure is of paramount importance. This necessitates a conservative reservoir regulation approach, which includes operating reservoirs at lower than normal water levels[25,26], implementing pre-release of volume prior to the flood season[27,28], and assuring the maintenance of flood protection facilities. Although these measures might reduce the water supply of irrigation and civil usage as well as the power generation, the trade-offs are indispensable in avoiding disasters. Such a conservative strategy not only enhances the system's resilience to hydrological extremes, but also markedly reduces the risk of overtopping when operational norms may be impacted by external forces.

The destruction of Kakhovka dam has caused a substantial decrease in usable volume in the Dnipro cascade, which underscored the urgent need for a reevaluation of the cascade regulation rules[29]. Special attention should be paid on Kremenchuk, the reservoir with the largest usable volume and the only remaining facility with annual regulation ability [30] along the Dnipro cascade. Given its position as the third among five existing reservoirs, it is particularly vulnerable and cannot afford any mishap. The Zaporizhzhya Nuclear Power Plant (ZNPP), which was dependent on the Kakhovka reservoir for coolant water, is another critical concern. It has been disconnected due to low water levels, and although the coolant water pool of ZNPP remains relatively stable in the shutdown state[31], it would be safer to compensate for water loss via the original Dnipro river channel using temporary pipelines. As an ancillary measure, the enhancement of hydrological monitoring and forecasting capabilities[32,33] might help facilitate optimal utilization of the remaining volumes within the ideal framework of conservative regulation.

Conclusion

Our study highlights the value of remote sensing in identifying operational anomalies and predicting early warning signs in water resource infrastructure, which can enable the development of effective mitigation strategies.

As satellite data accessibility improves, we are advancing toward near real-time, high-resolution remote monitoring of both water quantities and qualities in rivers[34,35], lakes[36–38], and reservoirs[39–42]. Data assimilation in conjunction with meteorological and hydrological models[43–46] can further enhance the dynamic simulation of water resources and infrastructure operations, paving the way for a more comprehensive and nuanced understanding of water system behaviors and vulnerabilities.

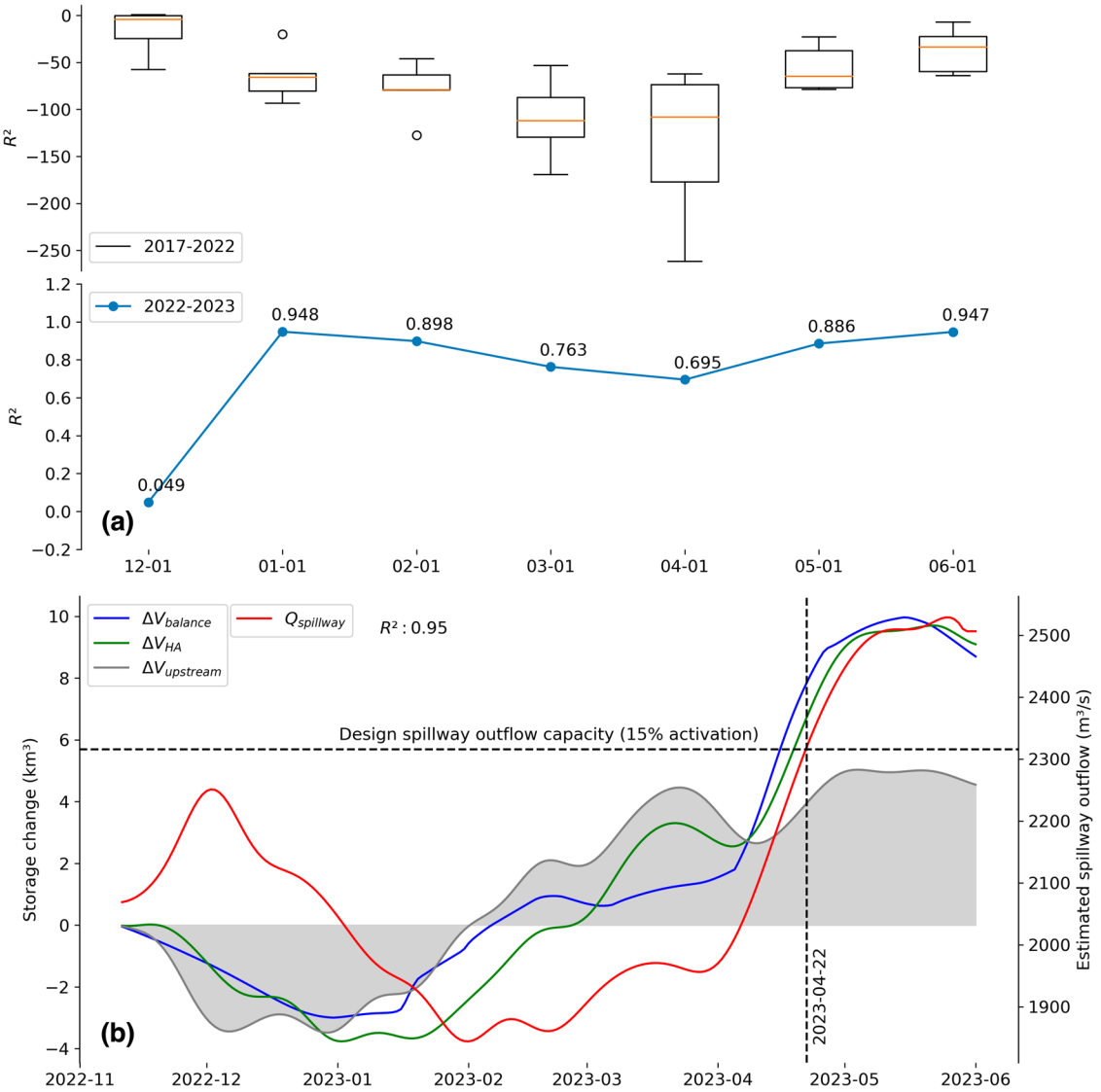

Fig. 3 | Reservoir unregulated outflow hypothesis test and storage change simulation. a Non-regulated outflow hypothesis test metrics, measured by the coefficient of determination. The upper subplot presents the boxplot of metrics for 2017–2022, while the lower subplot depicts the same for 2022–2023. The start date for all tests is November 11, with end dates indicated on the *x* axis. **b** Storage change and outflow simulation for the period from November 2022 to June 2023. $\Delta V_{balance}$ and ΔV_{HA} represent the simulated and remotely sensed storage change of the Dnipro cascade, respectively, while $\Delta V_{upstream}$ corresponds to the remotely sensed storage change for five upstream reservoirs. On 2023-04-22, the estimated outflow exceeded the design capacity of the spillway that was activated. Refer to "Methods" for further details.

Table 1 | Safety checkpoints with the corresponding risk conditions and mitigation measurements

Checkpoint	Risk conditions or danger signs	Water level	Probability of or remain overtopping in next month (PO)	Proposed mitigation plan at minimum (MM)	PO after MM
2022-11-11	Three sluice gates damage	15.25 m	0.35%	Restore spillway gates	0.014%
2023-01-31	Low water level Anomalous spillway activation	14.13 m	0.11%	Restore spillway gates Check available gates	0.014%
2023-02-28	Anomalous spillway activation	14.41 m	0.93%	Maintenance Water-level regulation	0.18%
2023-03-31	Water level rising Anomalous spillway activation	14.74 m	23%	Personnel on duty Activate 50% of spillway	2.4%
2023-04-23	Overtopping Anomalous spillway activation	16.59 m	79%	Activate all spillway Issue flood warning	7.6% if 50% activate
2023-05-28	Ancillary structures destructing Overtopping Anomalous spillway activation	17.34 m	45%	Activate all spillway Evacuation	1.6% if 50% activate

Beyond our technological advancements lies an urgent societal call: the imperative of transparent data sharing, especially concerning public water infrastructure. As our study on the Kakhovka Dam underscores, this transparency is pivotal at the watershed scale, where potential cascading impacts arise from interconnected systems. Open access to regional data, encompassing design parameters, and both remote and in-situ monitoring, not only accelerates the development and refinement of scientific methodologies but also ensures more accurate predictions of water system behavior. In turn, this fosters the establishment of proactive water hazard mitigation strategies, safeguarding the longevity and safety of our water systems.

Methods

Spillway activation monitoring

The activation of a spillway is a key measure for flood mitigation in reservoirs. Specifically, at the Kakhovka Dam, the activation of its top flow-type spillway is effectively monitorable using remote sensing data. In this study, we tracked the percentage of spillway activation by analyzing multisource optical images from 2017 to 2023.

Optical images from PlanetScope, Sentinel-2, and Landsat-8 were used to analyze the spillway activation states. Table 2 summarizes each sensor's configuration and the number of clear images used in the study, after excluding those with cloud cover. Data availability covering the dam location is detailed in Supplementary Fig. 2.

We measured the percentage of spillway activation by relating the water splash width to the total length of the spillway on a daily scale from optical remote sensing images, as depicted in Fig. 1a. For dates lacking valid observations due to cloud coverage or data absence, we assumed that the activation state was identical to that of the previous date of valid record. Consequently, the spillway activation percentage remained at around 15% from late November 2022 until the dam's breach. Supplementary Fig. 3a–c demonstrates comparative visualization of PlanetScope, Sentinel-2, and Landsat dated 2023-03-22. There are also some snapshots of the spillway activation during normal flood mitigation periods, as depicted in Supplementary Fig. 3d–f.

The measurement's uncertainty primarily stems from two factors: sensor resolution and the dynamic nature of the water splash. With the spillway dam's total length being 435 m[23], the per-pixel measurement bias is ~0.7% for PlanetScope, 2.3% for Sentinel-2, and 6.9% for Landsat-8. High-resolution images from PlanetScope are most effective for assessing spillway activation, even under haze conditions (Supplementary Fig. 3a). While Landsat's medium resolution introduces a higher degree of uncertainty (Supplementary Fig. 3c), it is still valuable for confirming when gates are fully closed. The dynamic nature of water splash poses challenges for precise measurement, and its width may also correlate with the outflow rate, influenced by the reservoir's water level. However, these uncertainties do not impede the identification of operation anomalies in this case, as the same spillway activation condition remains consistent for over 6 months.

Outflow hypothesis test

Supplementary verification was required to substantiate the hypothesis of unregulated outflow given the remote sensing images' incapability to offer information regarding the vertical opening degree of the sluice gates and the operation state of the hydroelectric power station. We approximated the outflow through spillway using the equation of free flow through rectangular weir[47] as:

$$Q = N\frac{2}{3}c_d b 2g^{1/2}H^{3/2} \tag{1}$$

where N is the number of functioning gates, c_d is the contraction coefficient, b is the width of the gate, g is gravity acceleration constant, and H is the head difference between the upstream and downstream water levels.

Assuming in the period of unregulated outflow, all parameters other than H are constant, by incorporating the design discharge capacity of spillway outflow[23] $Q_{design} = 15{,}438\ m^3\ s^{-1}$ and percentage of spillway activation $P_{activate}$, we deduced:

$$Q = 15438 \times P_{activate}\left(\frac{H}{H_{design}}\right)^{3/2} \tag{2}$$

Where H_{design} is the design water head.

To simplify, we assumed that the water head difference is proportional to water level of the reservoir, thus utilized the water level from altimetry product to approximate H, meaning H_{design} is a parameter in need of calibration.

After fixing the H_{design}, we could pinpoint the estimated start date of spillway overflow from reservoir water level time series.

We validated the hypothesis based on water balance of the Dnipro cascades, represented by the following equation:

$$V^t_{balance} = V^{t-1}_{balance} + (Q^t_{inflow} - Q^t - Q^t_{usage})\Delta t \tag{3}$$

where $V^t_{balance}$ is the estimated cascade volume in time t. Q is the outflow through spillway, Q_{inflow} is the streamflow, and Q_{usage} represents water usage, including irrigation and civil water usage, taken from the cascade storage, assumed as a constant value, which is also a parameter in need of calibration.

Given the absence of streamflow observation data for the Dnipro River, we sourced daily discharge simulation data for the site of the Kakhovka Dam from GloFAS-ERA5[45], which have accounted the reservoir evaporation in the reservoir module, spanning the period from 1979 to 2023. We then refined the annual flow volume by implementing quantile mapping, based on the specific annual streamflow volume and corresponding reliability values stipulated in an evaluation report[29].

We further calculated the remotely sensed cascade storage time series as:

$$V^t_{HA} = V^{t-1}_{HA} + \sum_{i=1}^{6}(H^t_i - H^{t-1}_i)\cdot(A^t_i + A^{t-1}_i)/2 \tag{4}$$

Where H^t_i and A^t_i is the water level and surface extent area of the ith reservoir of the Dnipro cascade at time t.

We set the initial storage values to zero for both the estimated and remotely sensed storage time series at the starting step. Then, we test the unregulated outflow hypothesis by computing the coefficient of determination between the two time series.

For consistency, we leverage the Area-Elevation (A–E) relationship to determine the reservoir surface area based on the water level. The water levels were collected from the Global Reservoir and Lake Monitor (G-

Table 2 | Optical images used for spillway activation monitoring

Sensors	Spatial resolution for RGB	Typical temporal frequency	Original source	Number of clear images examined
PlanetScope	3 m	Daily	Planet Labs PBC	1005
Sentinel-2	10 m	5 days	European Space Agency	428
Landsat-8	30 m	16 days	U.S. Geological Survey	145

REALM) dataset[48]. We bridged the 7–10 days temporal resolution gap in G-REALM's point data by applying cubic spline interpolation, followed by a 7-day moving average to create a smooth, continuous water level time series. The reservoir water surface area was determined using multisource remote sensing data, with optical data primarily delineating surface water boundaries and Synthetic Aperture Radar (SAR) imagery compensating for areas obscured by clouds. Water surface extent was extracted from optical images using a supervised classification method based on water indices[49], supplemented by manual refinement, while SAR images were processed with an automated algorithm named RAPID[2,3]. The SAR images used in this study are the Radiometrically Terrain Corrected Sentinel-1 products at, C-band, dual-polarization, and 10-m resolution from Alaska Satellite Facility. Supplementary Table 1 presents the water levels and corresponding surface areas for the Dnipro cascade, derived from remote sensing data.

The test period commences on November 11, 2022, and concludes on the first day of each subsequent month through June. We applied the hypothesis test for each time period from 2017 to 2023 for comparison, constraining H_{design} and Q_{usage} as [15.8, 17.4] m and [20, 100] $m^3 s^{-1}$, respectively, and calibrated them by minimizing the Root Mean Squared Error between $V^t_{balance}$ and V^t_{HA}. For the percentage of spillway activation, we use the measured value 15% from "Spillway activation monitoring" to implement our primary test (Fig. 3). To ensure the reliability of our conclusions, we also incorporated a sensitivity analysis by varying the spillway activation percentage from 10% to 20% and evaluating the implications for both the storage time series and the overflow start date.

Supplementary Fig. 4a reveals that unregulated outflow is plausible when spillway activation ranges from 13.8 to 17.5%, which corresponds to about 4–5 sluice gates remaining open. The inferred onset of overflow falls between April 19, 2023, and May 9, 2023 (Supplementary Fig. 4b), is consistent with the initial overtopping observed from remote sensing image (Fig. 2d).

Key uncertainties in this section, including the spillway activation percentage, inflow simulation from GloFAS-ERA5, and the A–E curve derived from remote sensing data, were thoroughly examined. The first uncertainty was directly assessed through a comprehensive sensitivity analysis. The simulation streamflow has demonstrated commendable performance against observation at locations near the site of Kakhovka[45], and the values were further adjusted using quantile mapping based on localized statistics, bolstering their reliability as proxy of the inflow. G-REALM data is known to exhibit minimal bias for large reservoirs (<10 cm)[50], indicating that the principal challenge stems from its relatively low temporal resolution, which could influence the accuracy of the reservoir storage retrieval. Given the study area's stable terrain, reservoir storage is more influenced by water levels than by surface area, reducing the effect of area measurement errors. Although G-REALM captured water level for every 7–10 days, and the trapezoidal cross-section assumption introduced some level of uncertainty, the extended test period and high monthly R-squared values lend credence to our results. These findings demonstrate that, despite the inherent uncertainties from multisource input data, the assumption of unregulated outflow remains a valid and well-supported hypothesis.

Estimation of overtopping probability

Inspired by Stefanyshyn and Benatov[51], we define the occurrence of overtopping in the Kakhovka reservoir as a sign of danger. We estimate the probability of overtopping[52] in the subsequent time step by taking into account the stochastic nature of the inflow and the reservoir's current state:

$$P_f = P(H^{t+1} \geq H_o) = P(Q^{t+1}_{inflow} \geq Q + (H_o - H^t) * (A_o + A^t)/2/\Delta t) \tag{5}$$

Where H_o is the water level that triggers overtopping, A_o is the corresponding water extent, and Q is the current maximum available outflow capacity.

We investigate the probability of overtopping in the subsequent time step, considering two scenarios of outflow capacity: the actual capacity without any mitigation, as estimated from remote sensing imagery, referred to as the "probability of overtopping" (PO), and the capacity after applying proposed minimal mitigation measures, termed "PO after MM", as detailed in Table 1.

We designate the 99th percentile of the historical water level, excluding the years 2022 and 2023 as the H_o(equal to 16.56 m), and we retrieve A_o using the A–E relationship from "Outflow hypothesis test". Consequently, Eq. (5) simplifies to:

$$P_f = P\left(Q^{t+1}_{inflow} \geq f(\Delta t, Q) \right) \tag{6}$$

We then evaluate the possibility of overtopping at two scales, as

$$P_f = P(Q^{t+1}_{mean} \geq f(30, Q)) + P(Q \leq Q^{t+1}_{mean} < f(30, Q)\ Q^{t+1}_{\max 7} \geq f(7, Q)) \tag{7}$$

Here, Q^{t+1}_{mean} and $Q^{t+1}_{\max 7}$ denote the mean streamflow and maximum average streamflow within a 7-day window for the subsequent month, respectively.

We employ a Gaussian copula function[53] to determine the correlation of streamflow between successive months:

$$C(u, v, w) = \Phi_{\Sigma}(\Phi^{-1}(u), \Phi^{-1}(v), \Phi^{-1}(w)) \tag{8}$$

Where $C(u, v, w)$ represents the three-dimensional copula function, with variables u, v, and w denoting the transformed values obtained by applying the inverse of the cumulative distribution function to the observed data series of Q^t_{mean}, Q^{t+1}_{mean} and $Q^{t+1}_{\max 7}$, respectively.

We fit the copula function with refined discharge simulation described in "Outflow hypothesis test", excluding the data from 2022 and 2023. We employ a log-normal distribution as the marginal distribution function. Subsequently, we implement Markov Chain Monte Carlo sampling[54] of the conditional distribution presented in Eq. (7) to estimate the overtopping probability.

Resolving analytical uncertainties with next-gen remote sensing

The current landscape of widely accessible remote sensing data effectively facilitates the identification and analysis of notable operational anomalies within large water infrastructure projects. As remote sensing technology continues to evolve, it promises substantial enhancements to this analytical process. High-resolution imagery, finer than 1 m, can swiftly pinpoint issues such as improper sluice gate operations or structural integrity losses, with the capability for optical detection or revealing internal damages via InSAR techniques[10]. In addition, the precision in monitoring reservoir storage is poised for improvement with the advent of new satellite altimetry missions like SWOT[50], or by integrating high-quality bathymetric data and increasing the frequency of shoreline measurements[55]. Moreover, incorporating data assimilation techniques with remotely sensed streamflow retrieval at lake[37] or river-reach[56] scales is expected to greatly enhance the precision of inflow estimates, thereby strengthening water resource management and hazard mitigation strategies. By harnessing these advanced satellite products and synchronizing them with engineering design parameters, the establishment of a globally comprehensive, remote sensing-based monitoring system becomes a tangible prospect.

Data availability

The Sentinel-2 and Landsat images used in this study are accessible at https://www.sentinel-hub.com/index.html. The PlanetScope images are obtained through https://www.planet.com/. The Sentinel-1 images were acquired from https://asf.alaska.edu/. The reservoir water levels can be found at https://ipad.fas.usda.gov/cropexplorer/global_reservoir/. The GloFAS-ERA5 river discharge reanalysis data are available at https://cds.climate.copernicus.eu/cdsapp#!/dataset/cems-glofas-historical?tab=overview. Underlying data for the main manuscript figures is included in csv

files, are available and can be accessed at https://doi.org/10.6084/m9.figshare.25403698.

Code availability

The computer code for the main methods described in this manuscript is available and can be accessed at https://doi.org/10.6084/m9.figshare.25403698.

Received: 25 October 2023; Accepted: 16 April 2024;
Published online: 02 May 2024

References

1. Shen, X., Wang, D., Mao, K., Anagnostou, E. & Hong, Y. Inundation extent mapping by synthetic aperture radar: a review. *Remote Sens.* **11**, 879 (2019).
2. Yang, Q. et al. A high-resolution flood inundation archive (2016–the present) from Sentinel-1 SAR Imagery over CONUS. *Bull. Am. Meteorol. Soc.* **102**, E1064–E1079 (2021).
3. Shen, X., Anagnostou, E. N., Allen, G. H., Robert Brakenridge, G. & Kettner, A. J. Near-real-time non-obstructed flood inundation mapping using synthetic aperture radar. *Remote Sens. Environ.* **221**, 302–315 (2019).
4. Tellman, B. et al. Satellite imaging reveals increased proportion of population exposed to floods. *Nature* **596**, 80–86 (2021).
5. He, K., Yang, Q., Shen, X. & Anagnostou, E. N. Brief communication: western Europe flood in 2021 – mapping agriculture flood exposure from synthetic aperture radar (SAR). *Nat. Hazards Earth Syst. Sci.* **22**, 2921–2927 (2022).
6. Cerrai, D., Yang, Q., Shen, X., Koukoula, M. & Anagnostou, E. N. Brief communication: Hurricane Dorian: automated near-real-time mapping of the 'unprecedented' flooding in the Bahamas using synthetic aperture radar. *Nat. Hazards Earth Syst. Sci.* **20**, 1463–1468 (2020).
7. Yang, Q. et al. Predicting flood property insurance claims over CONUS, fusing big earth observation data. *Bull. Am. Meteorol. Soc.* **103**, E791–E809 (2022).
8. Sheffield, J. et al. Satellite remote sensing for water resources management: potential for supporting sustainable development in data-poor regions. *Water Resour. Res.* **54**, 9724–9758 (2018).
9. Ma, P. et al. Toward Fine Surveillance: a review of multitemporal interferometric synthetic aperture radar for infrastructure health monitoring. *IEEE Geosci. Remote Sens. Magaz.* **10**, 207–230 (2022).
10. Milillo, P. et al. Monitoring dam structural health from space: Insights from novel InSAR techniques and multi-parametric modeling applied to the Pertusillo dam Basilicata, Italy. *Int. J. Appl. Earth Obs. Geoinf.* **52**, 221–229 (2016).
11. Xiao, R., Jiang, M., Li, Z. & He, X. New insights into the 2020 Sardoba dam failure in Uzbekistan from Earth observation. *Int. J. Appl. Earth Obs. Geoinf.* **107**, 102705 (2022).
12. Abnett, K. Ukraine says Kakhovka Dam collapse caused 1.2 billion euros in damage. *Reuters* https://www.reuters.com/world/europe/ukraine-says-kakhovka-dam-collapse-caused-12-billion-euros-damage-2023-06-20/ (2023).
13. DPA WORLD. At least 62 people dead after floods unleashed by Kherson Dam Breach. *anews* https://www.anews.com.tr/world/2023/06/21/at-least-62-people-dead-after-floods-unleashed-by-kherson-dam-breach 2023)
14. Mykhaylov, I. What does the destruction of Kakhovka Hydroelectric Station mean for Ukraine agriculture? *Successful Farming* https://www.agriculture.com/news/business/what-does-the-destruction-of-kakhovka-hydroelectric-station-mean-for-ukraine (2023).
15. Telishevska, S. Reconstruction of the Kakhovka HPP will last 5 years and will cost up to $1 billion. *babel* https://babel.ua/en/news/94763-reconstruction-of-the-kakhovka-hpp-will-last-5-years-and-will-cost-up-to-1-billion (2023).
16. Shumilova, O. et al. Impact of the Russia–Ukraine armed conflict on water resources and water infrastructure. *Nat. Sustain.* **6**, 578–586 (2023).
17. Brumfiel, G. Russia is draining a massive Ukrainian reservoir, endangering a nuclear plant. *NPR* (2023).
18. Рогов. В Запорожье заявили об угрозе прорыва дамбы из-за уровня воды в водохранилище. *lenta.ru* https://lenta.ru/news/2023/05/04/voda_voda/ (2023).
19. Hill, E. New satellite imagery of the Khakovka dam from June 5 shows evidence that a section of the roadway and sluice gates had been recently damaged or destroyed.(Left: May 28, Right: June 5): @Maxar pic.twitter.com/o6StIwloJr. *Twitter* https://twitter.com/evanhill/status/1665933276647772160 (2023).
20. Graham, J. R., Creegan, P. J. & Hamilton, W. S. Erosion of concrete in hydraulic structures. *ACI Mater. J.* **84**, 136–156 (1987).
21. Heidarzadeh, M. & Feizi, S. A cascading risk model for the failure of the concrete spillway of the Toddbrook dam, England during the August 2019 flooding. *Int. J. Disaster Risk Reduct.* **80**, 103214 (2022).
22. Goodling, P. J., Lekic, V. & Prestegaard, K. Seismic signature of turbulence during the 2017 Oroville Dam spillway erosion crisis. *Earth Surf. Dyn. Discuss*. **6**, 351–367 (2018).
23. Обухов, Є. В. Каховському водосховищу-55 років. Український гідрометеорологічний журнал **10**, 116–125 (2012).
24. Ставская, Я. Не удается удерживать уровень Днепра: в КГГА объяснили причины потопа в Киеве. Информационное агентство https://www.unian.net/society/navodnenie-v-kieve-chto-stalo-prichinoy-zatopleniy-kgga-novosti-kieva-12225417.html (2023).
25. Zhou, Y., Guo, S., Liu, P. & Xu, C. Joint operation and dynamic control of flood limiting water levels for mixed cascade reservoir systems. *J. Hydrol.* **519**, 248–257 (2014).
26. Jiang, H., Yu, Z. & Mo, C. Reservoir flood season segmentation and optimal operation of flood-limiting water levels. *J. Hydrol. Eng.* **20**, 05014035 (2015).
27. Hossain, M. S., Nair, M., Mohd Sidek, L. & Marufuzzaman, M. A pre-release concept for reservoir management and the effect analysis on flood control. In *ICDSME 2019* 556–566 (Springer Singapore, 2020).
28. Wei, G. et al. Deriving optimal operating rules for flood control considering pre-release based on forecast information. *J. Hydrol.* **615**, 128665 (2022).
29. Обухов, Е. В. Внешний водообмен на днепровских водохранилищах в проектных и современных их параметрах с учетом водности года. Гідроенергетика України **1-2**, 23 (2020).
30. Khilchevskyi, V., Grebin, V., Dubniak, S., Zabokrytska, M. & Bolbot, H. Large and small reservoirs of Ukraine. *J. Water Land Dev.* https://doi.org/10.24425/jwld.2022.140379 (2022).
31. Aszódi, A. The destruction of the Kakhovka Dam may have made it impossible to restart ZNPP for a longer period. *euronuclear* https://www.euronuclear.org/blog/the-destruction-of-the-kakhovka-dam-may-have-made-it-impossible-to-restart-znpp-for-a-longer-period/ (2023).
32. Yang, S., Yang, D., Chen, J. & Zhao, B. Real-time reservoir operation using recurrent neural networks and inflow forecast from a distributed hydrological model. *J. Hydrol.* **579**, 124229 (2019).
33. Zhao, T., Yang, D., Cai, X., Zhao, J. & Wang, H. Identifying effective forecast horizon for real-time reservoir operation under a limited inflow forecast. *Water Resour. Res*. **48**, W01540 (2012).
34. Lin, P. et al. Inversion of river discharge from remotely sensed river widths: a critical assessment at three-thousand global river gauges. *Remote Sens. Environ.* **287**, 113489 (2023).
35. Riggs, R. M. et al. Extending global river gauge records using satellite observations. *Environ. Res. Lett.* **18**, 064027 (2023).
36. Yao, F. et al. Satellites reveal widespread decline in global lake water storage. *Science* **380**, 743–749 (2023).

37. Riggs, R. M., Allen, G. H., Brinkerhoff, C. B., Sikder, M. S. & Wang, J. Turning lakes into river gauges using the LakeFlow algorithm. *Geophys. Res. Lett*. **50**, e2023GL103924 (2023).
38. Sagan, V. et al. Monitoring inland water quality using remote sensing: potential and limitations of spectral indices, bio-optical simulations, machine learning, and cloud computing. *Earth Sci. Rev.* **205**, 103187 (2020).
39. Li, Y., Zhao, G., Allen, G. H. & Gao, H. Diminishing storage returns of reservoir construction. *Nat. Commun.* **14**, 3203 (2023).
40. Gao, H., Birkett, C. & Lettenmaier, D. P. Global monitoring of large reservoir storage from satellite remote sensing. *Water Resour. Res*. **48**, W09504 (2012).
41. Wang, Y., Long, D. & Li, X. High-temporal-resolution monitoring of reservoir water storage of the Lancang-Mekong River. *Remote Sens. Environ.* **292**, 113575 (2023).
42. Das, P. et al. Reservoir Assessment Tool 2.0: stakeholder driven improvements to satellite remote sensing based reservoir monitoring. *Environ. Modell. Softw.* **157**, 105533 (2022).
43. Zhou, X., Revel, M., Modi, P. & Shiozawa, T. Correction of river bathymetry parameters using the stage–discharge rating curve. *Water Resour*. **58**, e2021WR031226 (2022).
44. Durand, M., Gleason, C. J. & Pavelsky, T. M. A framework for estimating global river discharge from the Surface Water and Ocean Topography satellite mission. *Water Resour*. **59**, e2021WR031614 (2023).
45. Harrigan, S. et al. GloFAS-ERA5 operational global river discharge reanalysis 1979–present. *Earth Syst. Sci. Data* **12**, 2043–2060 (2020).
46. Han, Z. et al. Improving reservoir outflow estimation for ungauged basins using satellite observations and a hydrological model. *Water Resour. Res*. **56**, e2020WR027590 (2020).
47. Kindsvater, C. E. & Carter, R. W. Discharge characteristics of rectangular thin-plate weirs. *J. Transp. Eng.* **124**, 772–801 (1959).
48. Birkett, C. M., Ricko, M., Beckley, B. D., Yang, X. & Tetrault, R. L. G-REALM: a lake/reservoir monitoring tool for drought monitoring and water resources management. Abstract [H23P-02] presented at 2017 AGU Fall Meeting, 11-15 Dec (2017).
49. Feyisa, G. L., Meilby, H., Fensholt, R. & Proud, S. R. Automated water extraction index: a new technique for surface water mapping using Landsat imagery. *Remote Sens. Environ.* **140**, 23–35 (2014).
50. Birkett, C. M., O'Brien, K., Kinsey, S., Ricko, M. & Li, Y. Enhancement of a global lake and reservoir database to aid climate studies and resource monitoring utilizing satellite radar altimetry. *J. Great Lakes Res.* **48**, 37–51 (2022).
51. Stefanyshyn, D. & Benatov, D. Application of a logical-probabilistic method of failure and fault trees for predicting emergency situations at pressure hydraulic facilities (the case of Kakhovka hydroelectric complex). Восточно-Европейский журнал передовых технологий **4**, 55–69 (2020)
52. Mo, C.-X. et al. A quantitative model for danger degree evaluation of staged operation of earth dam reservoir in flood season and its application. *Water Sci. Eng.* **11**, 81–87 (2018).
53. Renard, B. & Lang, M. Use of a Gaussian copula for multivariate extreme value analysis: some case studies in hydrology. *Adv. Water Resour.* **30**, 897–912 (2007).
54. Stuart, A. M., Voss, J. & Wilberg, P. Conditional path sampling of SDEs and the Langevin MCMC method. *Commun. Math. Sci.* **2**, 685–697 (2004).
55. Li, Y., Gao, H., Zhao, G. & Tseng, K. H. A high-resolution bathymetry dataset for global reservoirs using multi-source satellite imagery and altimetry. *Remote Sens. Environ*. **244**, 111831 (2020).
56. Wu, W.-Y., Yang, Z.-L., Zhao, L. & Lin, P. The impact of multi-sensor land data assimilation on river discharge estimation. *Remote Sens. Environ.* **279**, 113138 (2022).

Acknowledgements

The authors are grateful to Sergey Kravtsov from the University of Wisconsin-Milwaukee for his help in looking up the requisite Kakhovka Dam design parameters in Ukrainian and Russian scientific literature. This study is supported by the National Oceanic and Atmospheric Administration (NOAA). NA22OAR4050676I and NA22OAR4320150 have supported Qing Yang. NA22OAR4050676I, NA22OAR4320150 and Wisconsin Sea Grant 90-2_R_RCE-22_Shen_XS, and National Science Foundation (NSF) 2225076 have supported Xinyi Shen. NA20OAR4600288, NA22NES4050009I, NA22NES4050012D, NA22OAR4050676I, and NA19NES4320002 have supported Qingyuan Zhang. The manuscript's contents are solely the opinions of the authors and do not constitute a statement of policy, decision, or position on behalf of NOAA or any US government. The authors would like to acknowledge the valuable support of Planet Labs PBC in providing the high-resolution images used in this study. The authors thank the editor and the reviewers for their constructive and helpful comments to help us improve this study.

Author contributions

Q.Y.: conceptualization, methodology design, data analysis, writing, and editing; X.S.: conceptualization, review of data and methodology, writing, editing, funding acquisition, and supervision; K.H.: data analysis and manuscript revision; Q.Z.: data interpretation, review of methodology, writing, and editing; S.H.: program management, supervision, and resource facilitation; W.S. III: insights on incident attribution, analysis review, and manuscript editing; J.M.K.: data analysis and resource facilitation; E.N.A.: supervision, funding acquisition, review, and editing.

Competing interests

The authors declare no competing interests.

Additional information

Supplementary information The online version contains supplementary material available at https://doi.org/10.1038/s43247-024-01397-5.

Correspondence and requests for materials should be addressed to Xinyi Shen.

Peer review information *Communications Earth & Environment* thanks Yusupujiang Aimaiti and the other, anonymous, reviewer(s) for their contribution to the peer review of this work. Primary Handling Editors: Carolina Ortiz Guerrero. A peer review file is available.